MCB
Journals.ASM.org

129-Derived Mouse Strains Express an Unstable but Catalytically Active DNA Polymerase Iota Variant

Said Aoufouchi,[a] Annie De Smet,[b] Frédéric Delbos,[b]* Camille Gelot,[a] Ida Chiara Guerrera,[c] Jean-Claude Weill,[b] Claude-Agnès Reynaud[b]

Centre National de la Recherche Scientifique UMR 8200, Institut Gustave Roussy, Villejuif, and Université Paris-Sud, Orsay, France[a]; Institut Necker-Enfants Malades, INSERM U1151-CNRS UMR 8253, Sorbonne Paris Cité, Université Paris Descartes, Faculté de Médecine-Site Broussais, Paris, France[b]; Plateau Protéomes Necker, PPN, Université Paris Descartes, Structure Fédérative de Recherche Necker, Paris, France[c]

Mice derived from the 129 strain have a nonsense codon mutation in exon 2 of the polymerase iota (Polι) gene and are therefore considered Polι deficient. When we amplified *Polι* mRNA from 129/SvJ or 129/Ola testes, only a small fraction of the full-length cDNA contained the nonsense mutation; the major fraction corresponded to a variant *Polι* isoform lacking exon 2. *Polι* mRNA lacking exon 2 contains an open reading frame, and the corresponding protein was detected using a polyclonal antibody raised against the C terminus of the murine Polι protein. The identity of the corresponding protein was further confirmed by mass spectrometry. Although the variant protein was expressed at only 5 to 10% of the level of wild-type Polι, it retained *de novo* DNA synthesis activity, the capacity to form replication foci following UV irradiation, and the ability to rescue UV light sensitivity in *Polι*$^{-/-}$ embryonic fibroblasts derived from a new, fully deficient *Polι* knockout (KO) mouse line. Furthermore, *in vivo* treatment of 129-derived male mice with Velcade, a drug that inhibits proteasome function, stabilized and restored a substantial amount of the variant Polι in these animals, indicating that its turnover is controlled by the proteasome. An analysis of two xeroderma pigmentosum-variant (XPV) cases corresponding to missense mutants of Polη, a related translesion synthesis (TLS) polymerase in the same family, similarly showed a destabilization of the catalytically active mutant protein by the proteasome. Collectively, these data challenge the prevailing hypothesis that 129-derived strains of mice are completely deficient in Polι activity. The data also document, both for 129-derived mouse strains and for some XPV patients, new cases of genetic defects corresponding to the destabilization of an otherwise functional protein, the phenotype of which is reversible by proteasome inhibition.

The wide variety of DNA lesions originating from endogenous and exogenous DNA-damaging agents in living cells require responses that either directly reverse the DNA damage or temporarily enable it to be tolerated until DNA repair occurs. DNA repair and damage tolerance machineries are both required to overcome the many types of DNA damage encountered by a cell. The eukaryotic DNA damage tolerance pathway uses translesion synthesis (TLS), a process in which specialized DNA polymerases (Pols) copy DNA lesions that block progression of the replication fork.

TLS polymerases are found in organisms from all kingdoms of life. Most TLS polymerases are members of the Y family of DNA polymerases (1), a unique class of DNA polymerases that possess specialized structures that are adapted to accommodate the replication of damaged DNA substrates and, in some cases, to promote mutagenic DNA synthesis. Eukaryotic DNA polymerase members of the Y family include Rev1, Polκ, Polη, and Polι. Among these, Polι is present only in higher eukaryotes. A major characteristic of this protein is its very high error rate when copying *in vitro* template pyrimidines; G or T is preferentially incorporated rather than A opposite T in the template. However, Polι exhibits error-free replication on template purines (2–4). Interestingly, Polι exhibits different catalytic activities on both damaged and undamaged DNA when manganese is used as a cofactor instead of magnesium; these new activities include a dramatic increase in the ability of Polι to bypass DNA lesions (5). Thus, this property can be used as a marker for Polι activity *in vitro*. Until now, the physiological role of Polι has remained unknown. Polι has been implicated in mutagenesis in some situations and in error-free TLS in others (6–8). Several reports have proposed *POLI* as a candidate gene for the pulmonary adenoma resistance 2 (Par2) locus in mice (9–11). We and others have reported that Polι is involved in UV light-induced mutagenesis in Burkitt's lymphoma and xeroderma pigmentosum-variant (XPV) syndrome cell lines (12, 13). However, mice and humans lacking Polι tend to develop cancer at an increased rate, suggesting that Polι is not a major contributor to mutagenesis *in vivo* in the presence of other DNA repair and tolerance pathways (6–8, 11, 14).

Sequencing of *Polι* cDNA from several mouse strains has revealed the existence of several isoforms due to the presence of a large number of single nucleotide polymorphisms accompanied by amino acid substitutions and an elevated frequency of alterna-

Received 9 April 2015 **Returned for modification** 13 May 2015
Accepted 18 June 2015
Accepted manuscript posted online 29 June 2015
Citation Aoufouchi S, De Smet A, Delbos F, Gelot C, Guerrera IC, Weill J-C, Reynaud C-A. 2015. 129-derived mouse strains express an unstable but catalytically active DNA polymerase iota variant. Mol Cell Biol 35:3059–3070. doi:10.1128/MCB.00371-15.

Address correspondence to Said Aoufouchi, said.aoufouchi@gustaveroussy.fr.
* Present address: Frédéric Delbos, UMR 1064, Centre de Recherche en Transplantation et Immunologie, Université de Nantes, Nantes, France.

Supplemental material for this article may be found at http://dx.doi.org/10.1128/MCB.00371-15.

doi:10.1128/MCB.00371-15

tive splicing (9, 11). The 129-derived 129/SvJ and 129/Ola mouse strains possess a nonsense mutation in codon 27 of exon 2 in both alleles and have been reported to be naturally deficient in Polι (15). However, data from Gening and colleagues determined using a specific Polι activity assay suggested the presence of residual activity in brain extracts of 129-derived mouse strains (16).

Several groups have used these mouse strains as models to address the role of the enzyme *in vivo*. Such studies have shown that 129-derived mouse strains are more sensitive to urethane-induced lung adenoma (UILA) than other mouse strains, and their authors have suggested that Polι can act as a tumor suppressor (11). These strains are resistant to gamma irradiation-induced thymic lymphoma but sensitive to methylation agent-induced thymic lymphoma (17).

In the present work, we demonstrate that 129-derived mouse strains express a variant Polι protein lacking 42 amino acids encoded by exon 2. This is due to the removal of the premature termination codon (PTC) through the exclusion of exon 2, which contains the nonsense mutation. We also show that the expressed variant protein retains DNA polymerization activity in 129-derived cells and that, although the steady-state expression level of the variant protein is low, normal expression levels can be restored by treatment with the proteasome inhibitor Velcade, both *in vivo* and *in vitro*. We believe that these findings will lead to a reevaluation of the role of Polι using genuinely deficient mice.

MATERIALS AND METHODS

Cell culture. Fibroblast cell lines (XP6DU, XP70TMA, and XP31BE) were purchased from the Coriell Institute for Medical Research (Camden, NJ). XP11BR and immortalized fibroblasts from a healthy patient were obtained as a kind gift from Alain Sarasin (IGR, Villejuif, France). Fibroblasts from mice were immortalized using simian virus 40 (SV40) T-antigen transfection. HEK293T cells, MRC5 cells, and all fibroblasts were maintained in Dulbecco's modified Eagle's medium containing high glucose and GlutaMAX (Invitrogen, Carlsbad, CA) concentrations and supplemented with 10% fetal calf serum (FCS), 100 U/ml penicillin, and 100 U/ml streptomycin under 5% CO_2. Type I Burkitt's lymphoma BL2 cell lines were cultured in RPMI 1640 medium supplemented with GlutaMAX, 10% FCS (HyClone, Logan, UT), and penicillin-streptomycin (Invitrogen).

Construction of expression vectors. Full-length (FL) cDNA encoding wild-type (wt) Polι or variant Polι was obtained from RNA isolated from C57BL/6 and 129/Ola testis RNA, respectively, using reverse transcription-PCR (RT-PCR). PCR amplification was performed with Phusion DNA polymerase (Finnzymes), and the PCR product was cloned into the pCDNA expression vector or was fused to the N-terminal part of Polι using the pEGFP-C1 vector (Clontech) at the EcoRI site, which was rendered blunt ended using the Exo$^-$ Klenow fragment. The catalytic knockout mutant of the mouse *POLI* gene (Polι-cat^{KO}) was constructed using a QuikChange mutagenesis kit (Agilent Technologies). The following pair of primers was used for site-directed mutagenesis (the sites involved in the change are underlined): mIota D34A-1 (5′-GAGTCATAGTCCACGTAG CTCTGGATTGCTTTTATGC-3′) and mIota D34A-2 (5′-GCATAAAAG CAATCCAGAGCTACGTGGACTATGACTC-3′).

Sequencing of *Polι* mRNA from C57BL/6 and 129/Ola mice. Total RNA was extracted from testes using a Qiagen RNeasy kit and was reverse transcribed by random priming using a ProSTAR first-strand RT-PCR kit (Stratagene). The FL sequence encoding Polι was amplified using the following primers: iota-For (5′-CCATGGAGCCCTTGCACGC-3′) and iota-Rev (5′-TTATCTGTGCGCCGAGGG-3′). The exon 1-to-exon 3 fragment was amplified using primers iota-For and iota exon 3-Rev (5′-GTAGCGGCTCAGGTCTTCTCCG-3′) (35 cycles of 10 s at 98°C, 20 s at 67°C [for the FL sequence] or at 70°C [for the exon 1-to-exon 3 fragment], and 90 s at 72°C) and Phusion DNA polymerase. Amplified sequences were cloned using a Zero blunt ligation kit (Invitrogen), and DNA was extracted from 96 plasmids that tested positive and sequenced using an ABI Prism 3130xl genetic analyzer.

Quantitative PCR analysis. RNA was extracted and reverse transcribed as described above and then subjected to real-time quantitative PCR using TaqMan gene expression assays according to the instructions of the manufacturer and a Prism 7900 HT TaqMan instrument (Applied Biosystems). The mouse β2 microglobulin (β2m) gene (Mm00437762_m1) was used as a reference gene.

Antibody production. Anti-mouse Polι polyclonal rabbit antibody was raised against a 16-mer peptide (AEWERAGAARPSAHRC) corresponding to the C terminus of mouse Polι conjugated to keyhole limpet hemocyanin antigen. The specific antibody was affinity purified from sera using a peptide column (Custom Polyclonal Antibodies; Eurogentec).

Total extract preparation and immunoblotting. Whole-cell protein lysates were prepared as follows. Cell pellets were washed twice with cold phosphate-buffered saline (PBS) and incubated under conditions of agitation in a cold room for 20 min in radioimmunoprecipitation assay (RIPA) buffer (50 mM HEPES [pH 7.9], 150 mM NaCl, 1.25 mM EDTA, 0.1% SDS, 0.5% sodium deoxycholate, 1% NP-40, 1 mM dithiothreitol, 1× protease inhibitor mixture, 0.25 mM phenylmethylsulfonyl fluoride [PMSF]). Insoluble material was removed by centrifugation at 15,000 rpm at 4°C for 30 min. The protein concentration was determined using a bicinchoninic acid (BCA) protein assay kit (Thermo Fisher Scientific). Protein samples were mixed with Laemmli buffer and heated at 95°C for 5 min, resolved using SDS-PAGE, and transferred to nitrocellulose membranes. The membranes were then incubated with the appropriate antibodies and detected using chemiluminescence. The following antibodies were used: rabbit polyclonal anti-Polι antibody (see "Antibody production" above), mouse monoclonal anti-PCNA (Santa Cruz), goat polyclonal anti-GAPDH (anti-glyceraldehyde-3-phosphate dehydrogenase) (Abcam), rabbit polyclonal anti-beta actin (Abcam), rabbit polyclonal anti-green fluorescent protein (anti-GFP) (THE GFP antibody; GenScript), and rabbit polyclonal anti-Polη (Bethyl Laboratories).

Partial purification of the variant Polι isoform from whole-cell extracts of 129/Ola mouse testes. All operations were carried out at 2 to 4°C. Mouse testes were homogenized in a glass and Teflon homogenizer in five volumes of extraction buffer (20 mM Tris-HCl [pH 7.5], 2 mM dithiothreitol [DTT], 500 mM KCI, 0.5% NP-40, 5% glycerol, 5% sucrose, 1 mM PMSF, and protease inhibitor cocktail [Roche]). The homogenate was sonicated and centrifuged at 20,000 × *g* for 60 min, and proteins were separated using ammonium sulfate fractionation. The 35%-to-70% fraction containing Polι (as estimated using Western blot analysis) was subjected to chromatography using a G75 Sephadex column preequilibrated in buffer A (50 mM Tris-HCl [pH 7.5], 0.1 mM DTT, 1 mM EDTA, 25 mM NaCl, 0.5% NP-40, 5% glycerol). Fractions containing Polι (identified using Western blot analysis) were pooled and directly applied to a phosphocellulose column (P11) equilibrated with buffer A. After being washed with buffer A, the proteins on the column were eluted in one step using the same buffer supplemented with 300 mM NaCl. The protein eluate was dialyzed against buffer A for 5 h, and any remaining insoluble material was removed by centrifugation at 12,000 × *g* for 30 min. The protein solution was then recovered and loaded onto a fast protein liquid chromatography (FPLC) Mono S HR5/5 column (Pharmacia Biotech Inc.) that had been preequilibrated with buffer A containing 25 mM NaCl. Proteins were then eluted with a 25-ml linear gradient of NaCl (25 to 400 mM) in buffer A. Fractions that were recognized by the DNA Polι-specific antibody, which eluted at 200 to 220 mM NaCl, were pooled and dialyzed against buffer A containing 150 mM NaCl. The resulting fraction was immunoprecipitated using the anti-Polι antibody, which had been cross-linked to protein G-Sepharose following standard protocols. To perform isoelectric focusing (IEF), the immunoprecipitate was eluted from the Polι antibody-conjugated protein G-Sepharose beads for 30 min at room temperature using IEF buffer containing 9 M urea, 2% 3-[(3-cholamidopro-

pyl)-dimethylammonio]-1-propanesulfonate (CHAPS), 18 mM DTT, 0.001% bromophenol blue, and 0.5% IPG buffer (Amersham). After IEF, immobilized pH gradient (IPG) strips were equilibrated for 20 min in equilibration buffer (50 mM Tris-HCl [pH 8.8], 6 M urea, 30% glycerol, 65 mM DTT, 0.001% bromophenol blue) and then incubated in the same buffer containing 2.5% iodoacetamide. Afterwards, IPG strips were fixed in 10% SDS-PAGE gels using 0.5% agarose, followed by electrophoresis in the second direction.

In-gel digestion and MALDI-TOF analysis. After SDS-PAGE, the gels were silver stained using a mass spectrometry (MS)-compatible SilverQuest silver staining kit from Invitrogen. The area of the gel containing the protein of interest was excised and extracted, and the resulting peptides were separated using an UltiMate 3000 series HPLC system (Dionex). Ninety-six fractions were collected and analyzed using a model 4800 matrix-assisted laser desorption ionization–time of flight/time of flight (MALDI-TOF/TOF) analyzer (ABI). Spectral acquisition and processing were performed using 4000 series Explorer software (version 3.5.28193, build 1011; ABI) in positive reflection mode at fixed laser fluency with a low-mass gate and delayed extraction. External plate calibration was performed using 4 calibration points spotted throughout the plate. Additional internal calibration was performed using Glu-fibrinopeptide (m/z = 1,570.677). For each fraction, steps of 50 spectra in the range of 700 to 4,000 Da were acquired at a 200-Hz laser shot frequency. Five hundred spectra per sample were summed and processed to obtain monoisotopic values from isotope clusters exhibiting a raw spectrum signal-to-noise (s/n) ratio of 20. In each MS spectrum, the 8 most abundant peaks were selected for fragmentation, starting with the least abundant. One thousand tandem MS (MS/MS) spectra per precursor were summed in increments of 50. The resulting peak lists were submitted to an in-house Mascot (Matrix Science) version 2.2 search engine. UniProtKB/Swiss-Prot was used with *Mus musculus* as species selection. Parent and fragment mass tolerances were set to 20 ppm and 0.3 Da, respectively, and partial modification (oxidation) of methionines was allowed. A filter was applied to the search to reduce false positives and to match redundancies of the same peptide in several hits. A peptide score of greater than 20 and a false-discovery rate (FDR) of less than 1.5% were imposed. For all ambiguous results, the MS or MS/MS spectra were manually checked to ensure proper matching.

Turnover of endogenous variant Polι in mouse fibroblasts. Cells were treated with cycloheximide (50 μg/ml) for 3 h to block *de novo* protein synthesis and harvested at the indicated time points. Western blot analysis was conducted for Polι and a loading control (GAPDH [glyceraldehyde 3-phosphate dehydrogenase]), and densitometry analysis was performed. The ratios between the levels of Polι and GAPDH were then estimated.

Purification of ubiquitin conjugates. HEK293T cells were transfected with variant Polι-eGFP and His_6-ubiquitin expression vectors when indicated. Thirty-six hours posttransfection, MG 341 was added for 2 h before cell lysis and protein analysis. The cells were then lysed in 8 M urea–1% Triton X-100–0.1 M NaH_2PO_4–10 mM Tris-HCl [pH 8]–20 mM imidazole at room temperature. His-ubiquitin (Ub)-conjugated proteins were purified using nickel-nitrilotriacetic acid (Ni-NTA)–Sepharose beads (Qiagen). Ni-bound proteins were washed extensively with the same lysis buffer, and the beads were then washed three times with buffer [pH 6.3]. The proteins were then eluted in Laemmli loading buffer, resolved using SDS-PAGE, and analyzed using Western blotting.

DNA damage survival curves and killing assays. Fibroblasts from various mouse backgrounds were washed in PBS and then irradiated with UV-C (UVC) light or subjected to various DNA-damaging agents in the presence or absence of 1 mM caffeine. Following a 72-h incubation, the number of viable cells was determined by adding CellTiter 96 AQueous One solution (Promega) to the fibroblasts and incubating the resulting suspension for 4 h at 37°C. The absorbance was then measured at 490 nm. Background readings in the wells containing medium alone were subtracted from the sample well readouts. Survival is expressed as a percentage of the nonirradiated control value.

Focus detection. Human MRC5 fibroblast cells were transiently transfected with a wt Polι-enhanced GFP (eGFP)-expressing or variant Polι-eGFP-expressing plasmid. Thirty-six hours posttransfection, the cells were subjected to UVC irradiation at a dose of 20 J/m^2. To detect PCNA foci, both the irradiated and nonirradiated cells were first treated with cold CytoSKeleton (CSK) 100 buffer containing 10 mM piperazine-*N*,*N*′-bis(2-ethanesulfonic acid) (PIPES) (pH 6.8), 100 mM NaCl, 300 mM sucrose, 3 mM $MgCl_2$, 1 mM EGTA, 0.2% Triton X-100, antiproteases, and antiphosphatases for 5 min and then fixed in 4% paraformaldehyde (PFA). Endogenous PCNA foci (red) were detected by incubating the samples first for 1 h at room temperature with anti-PCNA antibodies (PC10; Santa Cruz) and then for 30 min at room temperature with anti-mouse antibody–Alexa Fluor 594. The coverslips were mounted using mounting medium (Dako) supplemented with DAPI (4′,6-diamidino-2-phenylindole) (Sigma). Fluorescence microscopy images were photographed at 6 h post-UV treatment. To determine the focus counts, at least 300 cells (containing more than 10 foci) were counted in three independent experiments.

In-gel DNA polymerase activity assay. A DNA polymerase activity gel assay was performed as described by Karawya et al. (18) with minor modifications. SDS-PAGE was conducted in the presence of 100 μg activated calf thymus DNA per ml, which was added prior to gel polymerization. Samples (100 μg of protein) were dissolved in sample buffer (50 mM Tris [pH 6.8], 5% glycerol, 0.67% SDS, 0.1 μM 2-mercaptoethanol, 0.33 mM EDTA, 0.002% bromophenol blue) but were not heated before loading onto 10% SDS-PAGE gels. The samples were electrophoresed in a cold room. The resulting gel was then washed four times in 250 ml of chilled renaturation buffer (50 mM Tris-HCl [pH 7.5]) on a shaker at 4°C for 1 h. Next, the gel was soaked for 4 h in 1 liter of Polι activity buffer containing 40 mM Tris-HCl (pH 7.5), 50 mM KCl, 0.075 mM $MnCl_2$, 2.5% glycerol, and 1 mM dithiothreitol. The gel was placed in a sealed box with activity buffer containing 1 mCi of [α-^{32}P]dCTP (3,000 Ci/mmol) per ml, and 13.3 μM (each) dATP, dTTP, and dGTP were added. The box was incubated at 37°C in an incubator for 16 h. To stop the reaction and remove unincorporated deoxynucleoside triphosphates (dNTPs), the gel was washed six times in 500 ml of chilled 5% trichloroacetic acid containing 1% sodium pyrophosphate on a shaker at 4°C for 16 h. The gel was then heat dried on Whatman 3MM paper (GE Healthcare Life Sciences) and analyzed by autoradiography.

Treatment of mice with Velcade. Wild-type (BALB/c) mice and variant Polι (129/Ola) mice (male, aged 16 to 24 weeks) were treated intravenously with Velcade (Janssen-Cilag) (1 mg/kg body weight). Mice were administered Velcade either once or twice (with the second administration performed after an interval of 72 h). At various times posttreatment, mice were sacrificed. Their testes were excised and homogenized in Laemmli buffer, sonicated to disrupt genomic DNA, and boiled for 5 min. The proteins were subsequently resolved using SDS-PAGE and analyzed using Western blot analysis.

RESULTS

Mouse strains derived from the 129 strain express exon 2-less *Polι* mRNA. Mouse strains derived from the 129 strain have been described as Polι deficient because they contain a homozygous single nucleotide polymorphism in exon 2 that changes the wild-type (wt) serine in codon 27, TCG, to an amber stop codon, TAG (15). However, when we reverse transcribed the RNA isolated from 129/SvJ or 129/Ola testes and amplified the full-length coding region using PCR, we obtained a fragment of a size similar to the size of the one amplified using RNA isolated from the C57BL/6 strain. Cloning and sequencing of the PCR products demonstrated that wt *Polι* mRNA was present in C57BL/6 cells and that a mixed sequence with and without exon 2 was present in 129/SvJ-

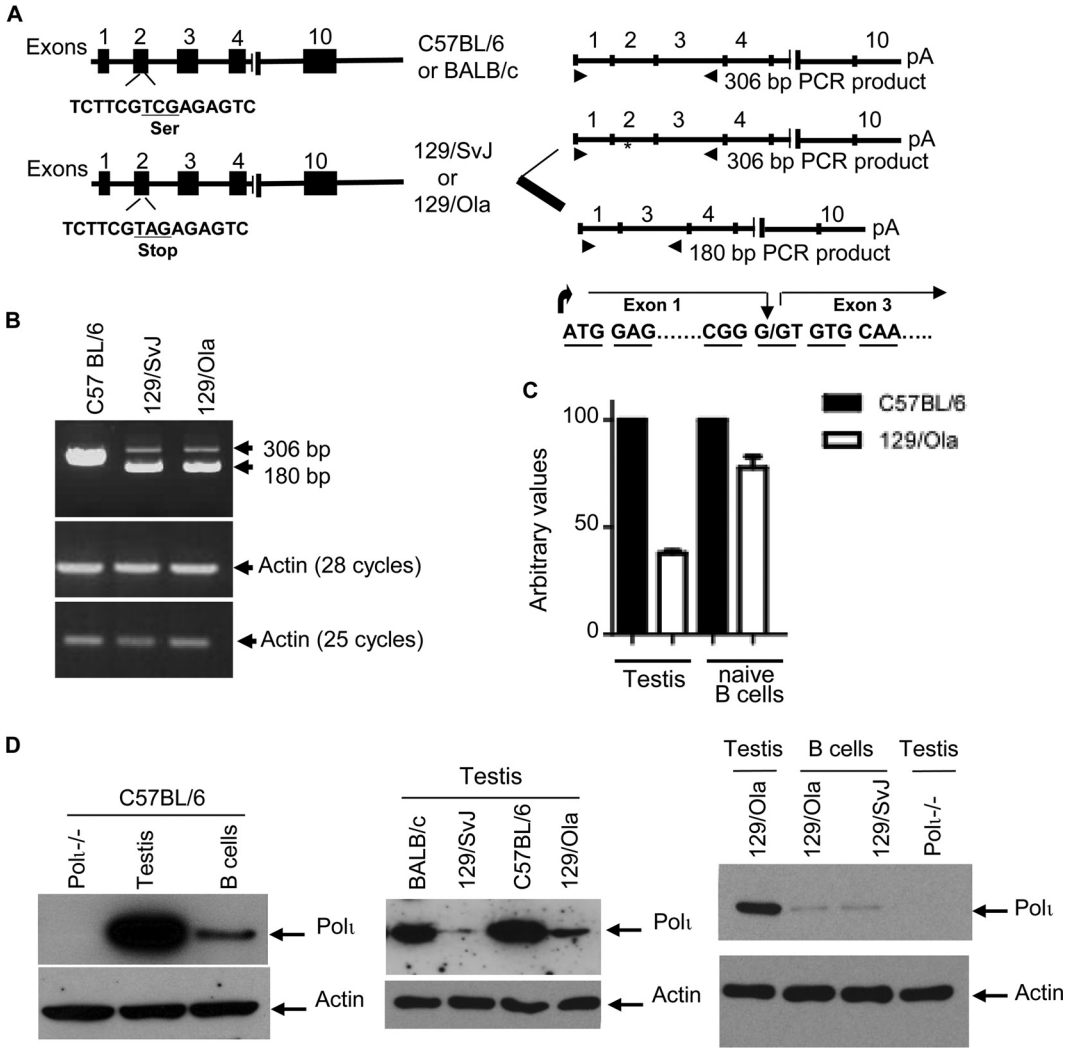

FIG 1 Mouse strains derived from the 129 strain express a *Polι* mRNA splicing variant lacking exon 2. (A) Schematic representation of genomic and mRNA structures of the mouse *POLI* gene. On the left, exons are indicated as black boxes, and the position of the stop codon in exon 2 is indicated. On the right, the positions of the PCR primers and the corresponding mRNA isoforms identified by PCR are indicated, as confirmed by sequencing. Sequencing revealed that the variant Polι isoform is caused by skipping exon 2 in frame, removing 126 bases (42 amino acids). (B) Total testis RNA purified from either C57BL/6- or 129-derived mouse strains was reverse transcribed using a random primer mix, and the region containing exons 1, 2, and 3 was PCR amplified from cDNA. PCR was performed with β-actin-specific primers to normalize for the amount of cDNA used. The position of the primers is indicated in panel A (right part). (C) The expression of *Polι* mRNA was analyzed in both testis cells and naive B cells using TaqMan real-time PCR, with primers located in the 3′ region of the mRNA, common to both forms of mRNA, relative to the housekeeping gene β*2m*, and the threshold cycle ($2^{-\Delta\Delta CT}$) method. mRNA expression is indicated using arbitrary values. Mean values are presented with error bars denoting ± standard deviations (SD) of the results of two independent experiments. (D) Polι protein expression analysis in both testis and B-cell extracts. Whole-cell lysates were prepared from testes and purified B splenocytes of the indicated mice strains, and the level of Polι expression was measured by immunoblotting using a rabbit anti-Polι antibody. Actin was used as a loading control. The specificity of the antibody was controlled using testes from Polι-deficient mice.

derived cells (see Fig. S1A in the supplemental material). The impact of the C-to-A mutation on mRNA splicing was further evaluated using primers located in exons 1 and 3 (Fig. 1A). Two PCR products, corresponding to one major band and one minor band, were amplified from 129-derived mouse strains (Fig. 1B). Sequence analysis of both fragments indicated that the major band (the shorter PCR product) lacked exon 2 (126 bp), resulting in an in-frame fusion of exons 1 and 3, whereas the minor band corresponded to a stop codon-containing sequence (see Fig. S1A). To estimate the abundance of each *Polι* RNA transcript, we cloned the product of the PCR and sequenced 100 clones containing an insertion. The sequencing results showed 71 clones representing the exon 2-less mRNA, 17 representing the full-length form containing the stop codon, and 12 containing unrelated sequences, which indicates that the exon 2-less *Polι* mRNA represents nearly 80% (71 of 88) of the Polι present in the testes of 129-derived mouse strains. In parallel, the level of mRNA expression *in vivo* was further quantified using quantitative RT-PCR in testes and naive splenic B cells. In this assay, exon 2-less *Polι* mRNA expression was 2.5-fold lower in testes from 129/Ola mice than in those from C57BL/6 mice but was only marginally (20 to 25%) lower than that of control B cells (Fig. 1C).

Mouse strains derived from the 129 strain express a variant Polι isoform lacking the exon 2-encoded domain. To investigate

whether *Polι* mRNA lacking exon 2 is translated into protein *in vivo*, we performed a Western blot analysis using a rabbit antibody raised against an 18-amino-acid peptide located at the C terminus of mouse Polι. This antibody should recognize both full-length Polι and the isoform lacking exon 2 (here termed variant Polι). A peptide competition assay was used to demonstrate that the antibody is highly specific for mouse Polι (data not shown). The specificity of the antibody was further confirmed by its lack of reactivity with respect to Polι-deficient samples from a mouse knockout (KO) line that we have established (see the description below) (Fig. 1D, left panel). Using this antibody, we next addressed the presence of the Polι variant in the tissues and cells of 129-derived mouse strains. Proteins from 129/SvJ, 129/Ola, or C57BL/6 mice were resolved using SDS-PAGE, and Polι was detected using immunoblotting. As shown in Fig. 1D (middle panel), testis extracts from C57BL/6 and BALB/c mice expressed, as expected, high levels of Polι protein, whereas testis extracts from both 129-derived strains expressed low but detectable levels of variant Polι. Similar results were obtained using protein extracts prepared from lipopolysaccharide (LPS)-activated splenic B cells (Fig. 1D, right panel). To provide further evidence for the presence of the variant Polι protein in 129-derived mouse strains, we performed an enrichment purification procedure so that the material could be identified using mass spectrometry (MS) (see Fig. S1A in the supplemental material). Total protein extracts from 129/Ola mouse testes were purified and immunoprecipitated using the anti-Polι antibody. The product was further fractionated using two-dimensional gel electrophoresis and then silver stained; after excision, the Polι polypeptide was extracted, and the protein was identified using mass spectrometry. Peptide mass mapping by MALDI-TOF/TOF clearly indicated that the protein corresponds to mouse Polι with high confidence (4 matching peptides and 8% sequence coverage [see Fig. S1B]). No information was obtained on the peptide sequence of the N terminus because none of the identified peptides matched this region. Together, these results unambiguously indicate that the stop codon is removed from the *Polι* transcript by an exon-skipping process in 129-derived mouse strains, thereby maintaining the open reading frame and leading to the expression of a variant Polι protein isoform lacking the 42 amino acids encoded by exon 2.

Exon 2 skipping alters variant Polι protein half-life. In 129-derived mouse strains, we observed that the levels of the *Polι* transcript (which is mainly represented by a splicing variant lacking exon 2) were lower in testis by a factor of only 2 to 2.5. Consequently, we hypothesized that the observed low levels of the variant Polι protein might result from increased proteasome-dependent degradation. We examined the effect of 26S proteasome inhibitor MG341 (Velcade) on turnover of the endogenous Polι variant. Mouse embryonic fibroblast (MEF) cells from 129/Ola mice were incubated with MG341, total protein extracts were prepared at various time points, and protein amounts were assessed based on Western blotting using the anti-Polι antibody. Incubation with MG341 resulted in a rapid stabilization of the variant isoform (Fig. 2A). Similar results were observed when HEK293T cells were transfected with wt or variant Polι-enhanced green fluorescent protein (eGFP) and incubated for 3 h with the proteasome inhibitor. As observed in 129-derived mouse cells, differences in the steady-state levels of the two proteins were readily apparent in transfected HEK293T cells in the absence of the proteasome inhibitor (Fig. 2B, left panel). To accurately quantify protein stabilization in the presence of MG341, SDS-PAGE and Western blotting analyses were performed with amounts of extracts from mutant-eGFP-transfected cells that were larger than those used with wt-eGFP transfection. The quantification analyses showed a 6-fold increase in the level of Polι variant protein in the presence of the proteasome inhibitor, but only a marginal increase was observed for the wt protein (Fig. 2B, right panel). Therefore, we conclude that the Polι-eGFP variant but not the wt protein is stabilized upon proteasome inhibition. To further analyze the stability of the variant Polι, we determined its half-life in the presence of cycloheximide (CHX), an inhibitor of *de novo* protein synthesis. The half-lives of wt Polι and variant Polι were determined in BL2 and HEK cells that had been stably transfected with the eGFP fusion constructs. After incubating the cell lines with CHX, we followed the protein decay at various time points using Western blotting and densitometric measurements. The results from the BL2 cell line are shown in Fig. 2C (left panel), and the quantification results presented in Fig. 2D reveal that the half-life of variant Polι is approximately 60 min; in contrast, no decay was observed for wt Polι during the 3-h experiment. Similar results were obtained upon transfection and CHX treatment of HEK293T cells with the wt and variant Polι-eGFP constructs (Fig. 2C, right panel). We can thus conclude that exon 2 deletion destabilized the endogenous and exogenous variant Polι proteins similarly and independently of the cell type used for transfection.

Polyubiquitylation targets mutant, damaged, and misfolded proteins for degradation by the proteasome. We decided to investigate whether the degradation of variant Polι occurs via polyubiquitylation. To do so, HEK293T cells were transfected with wt or variant Polι-eGFP together with a His_6-tagged ubiquitin expression vector. Thirty-six hours after transfection, the cells were incubated in the presence or absence of proteasome inhibitor for 3 h before harvesting. His-ubiquitylated (Ub) proteins were purified under denaturing conditions using Ni beads. His-Ub wt and variant Polι-eGFP levels were detected using an anti-eGFP antibody. Figure 2E shows that the variant isoform displayed steady-state polyubiquitylation that strongly increased after proteasome inhibition, while only a marginal fraction of the wt protein was polyubiquitylated in the presence of MG341. This result suggests that the exon 2-skipped mRNA encodes an unstable protein, the destabilization of which is mediated by polyubiquitylation and can be reversed by inhibition of the proteasome.

Velcade stabilizes the variant Polι protein *in vivo*. To assess the effect of proteasome inhibition on variant Polι protein stability *in vivo*, we used Velcade, an approved medical drug. For this experiment, 2- to 3-month-old 129/Ola male mice were intravenously administered identical doses of Velcade (1 mg/kg of body weight) (Fig. 2F retro-orbital venous sinus [left panel] and lateral tail vein [right panel]), either once or twice (with the second administration performed after a 3-day interval). The mice were sacrificed 24 h or 72 h after the final injection. Data presented in Fig. 2F indicate that the level of variant Polι was higher in the testes of Velcade-treated 129/Ola mice 72 h after either one or two injections than in the untreated BALB/c control mice. We observed no action of Velcade at 24 h following the administration of a single dose, indicating that the inhibition of 26S proteasome activity takes longer than 24 h to be observable *in vivo*. These results confirm and reinforce our findings reporting the expression of a Polι variant that lacks the domain encoded by exon 2 in 129-

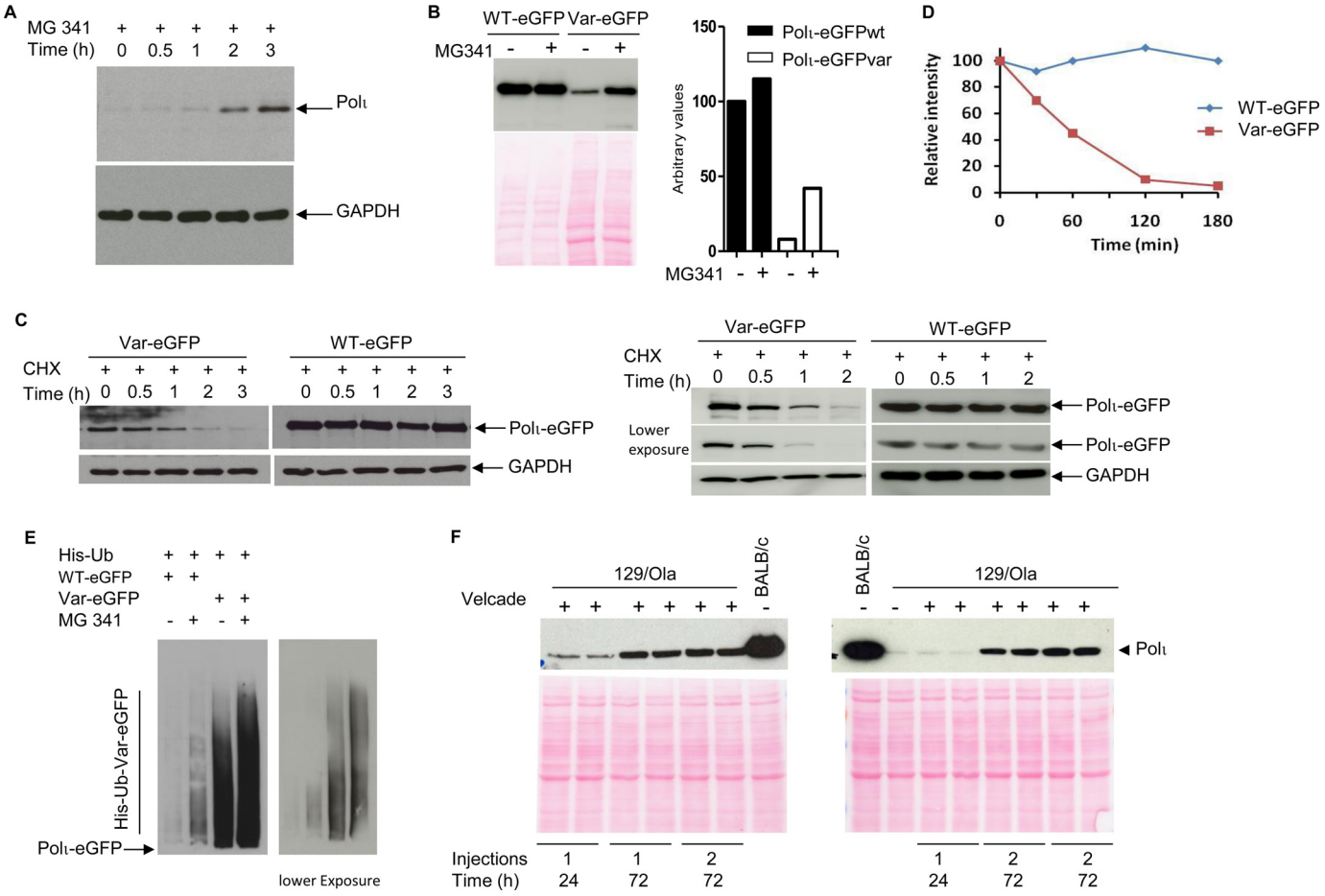

FIG 2 Absence of the exon 2-encoding domain increases proteasome-dependent turnover of variant Polι. (A) MEFs prepared from 129/Ola mice were incubated with MG341 to inhibit proteasome activity. Cell lysates obtained at the indicated time points were analyzed by immunoblotting using the anti-Polι antibody. GAPDH was used as a loading control. (B) HEK293T cells were transiently transfected with either the wt Polι-eGFP or variant (Var) Polι-eGFP expression vector. Forty-eight hours later, the cells were incubated for 3 h in the presence or absence of MG341. The expression levels of both proteins were monitored by immunoblotting using an anti-GFP antibody (5 μg of total protein for the wt and 25 μg for the Var-Polι were loaded on the gel and revealed by Ponceau S Red staining). (C) Stable BL2 (left) and HEK293T (right) clones expressing either wt Polι-eGFP or variant Polι-eGFP were incubated with cycloheximide (CHX; 50 μg/ml). At the indicated times, the level of Polι-eGFP expression was monitored by immunoblotting using an anti-GFP antibody. (D) Densitometric analysis of Polι-eGFP bands from the BL2 experiment. The protein levels are normalized to GAPDH. Mean values are presented with error bars denoting ± SD of the results of three independent experiments. (E) HEK293T cells were transfected with a variant Polι-eGFP expression vector and a plasmid encoding His_6-tagged ubiquitin (His-Ub). Forty-eight hours posttransfection, the cells were incubated in the presence or absence of MG341 for 3 h. His-tagged proteins were purified using nickel beads under denaturing conditions and then subjected to immunoblot analysis using an anti-GFP antibody. (F) Treatment of the mice with Velcade stabilizes the variant Polι protein. Strain 129/Ola mice were treated once or twice with injections of Velcade, either intraocularly (left panel) or in the tail vein (right panel). The mice were sacrificed at various time points posttreatment. Testis extracts were analyzed by SDS-PAGE using immunoblotting with anti-Polι antibody. The amount of protein analyzed, revealed by Ponceau S Red staining, is shown below the immunoblot.

derived mice strains and that its reduced accumulation is due to its targeting to the proteasome.

Sensitivity of Polι$^{-/-}$-expressing but not variant Polι-expressing fibroblasts to UVC irradiation. To assess the role of variant Polι in 129-derived cell lines, we established a complete *Polι* KO mouse strain. Embryonic stem (ES) cells having an inactivated *Polι* gene were identified in the GeneTrap ES cell database and were used to generate Polι-deficient animals, from which embryonic fibroblasts were isolated (see Fig. S4 in the supplemental material). We analyzed the cellular sensitivity of immortalized fibroblasts prepared from C57BL/6 (wt), 129/Ola, *Polη*$^{-/-}$ (19), or *Polι*$^{-/-}$ mice after exposure to increasing doses of UV-C (UVC) irradiation. As shown in Fig. S2A and B, only *Polη*$^{-/-}$ and *Polι*$^{-/-}$ fibroblasts exhibited significant sensitivity to UV irradiation (albeit to a lesser extent in the latter); fibroblasts of other genotypes, including 129/Ola cells, were insensitive. Interestingly, we showed that the sensitivity of both Polη- and Polι-deficient cells was enhanced by the addition of caffeine, an ATM- and/or ATR-dependent inhibitor of the infrared (IR)- and UV-induced DNA damage checkpoint. Remarkably, although expression of the variant Polι was low, the 129-derived fibroblasts were not UV sensitive, even in the presence of caffeine. Two hypotheses can explain this phenotype: first, UVC irradiation may either stabilize or increase the expression of variant Polι; second, because Polη is the major TLS polymerase involved in the UVC-induced DNA damage bypass pathway during the S phase, the absence of UV sensitivity of 129-derived fibroblasts may result from an increase in Polη expression that compensates for the low level of variant

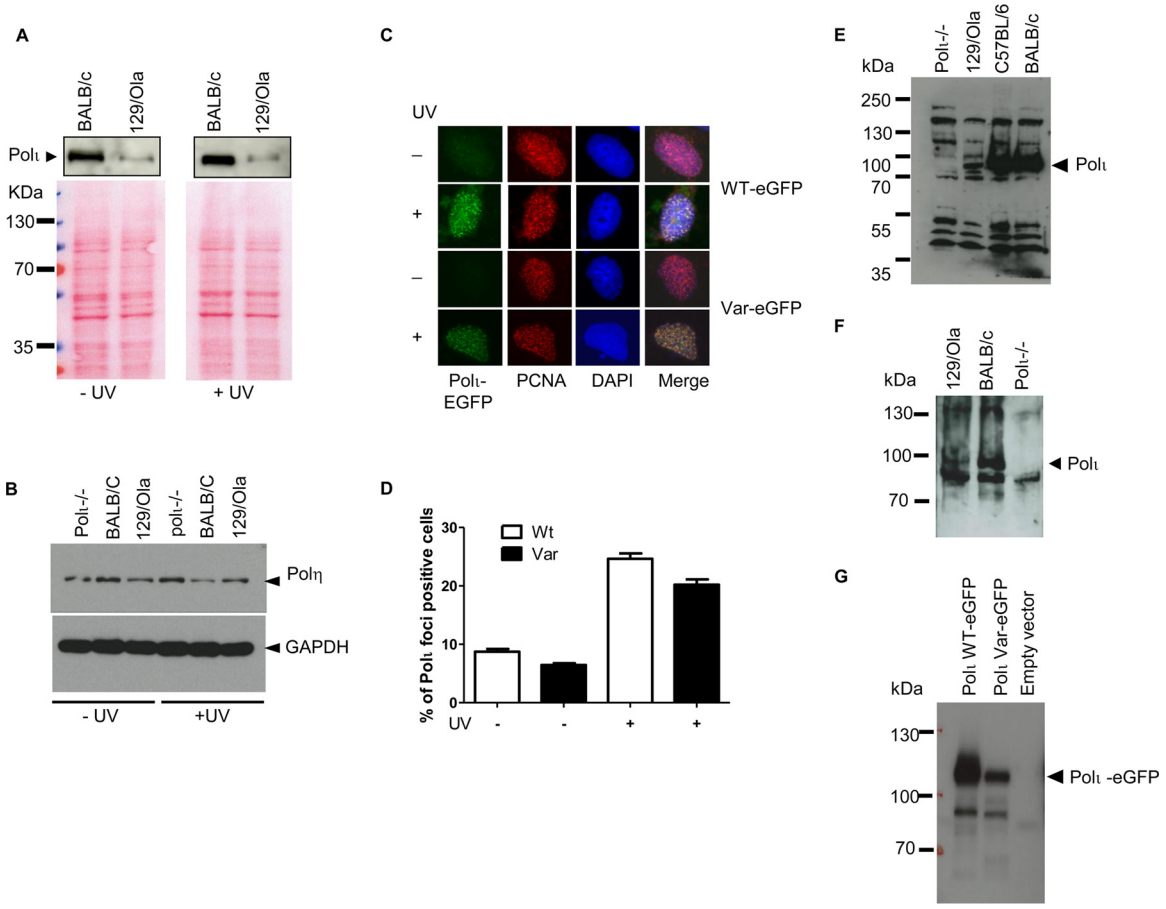

FIG 3 Variant Polι exhibits functional characteristics. (A and B) The expression of both Polι and Polη is not modified following UVC irradiation. Cell lysates prepared from fibroblasts with the indicated backgrounds were analyzed by immunoblotting using either an anti-Polι antibody (A) or anti-Polη antibody (B). Ponceau S Red or GAPDH staining was used as the protein loading control. (C) Normal MRC5 fibroblasts were transiently transfected with either wt Polι-eGFP or variant Polι-eGFP. Thirty-six hours later, the cells were irradiated with UVC (20 J/m^2) and incubated for 6 h. The cells were examined directly for epifluorescence (DAPI and Polι-eGFP) or analyzed for endogenous PCNA localization by indirect immunofluorescence. Cells with detergent-resistant Polι and PCNA staining were considered, and only cells displaying 10 foci or more were counted. (D) The values are presented as the means of the results of two independent experiments. At least 300 cells were counted per condition and experiment. (E, F, and G) Both endogenous and exogenous variant Polι retained the dNTP incorporation capacity as determined on the basis of an in-gel DNA polymerase activity assay. (E) Protein extracts from testes of the indicated mouse backgrounds were resolved on SDS-PAGE gels containing activated calf thymus DNA. Following in-gel protein renaturation, the capacity of the enzyme to incorporate dNTPs into DNA was assayed. (F) Data were determined as described for panel A, except that Polι was immunoprecipitated using the anti-Polι antibody prior to the in-gel DNA polymerase activity assay. (G) POLI KO fibroblasts were transfected with either wt Polι-eGFP or variant Polι-eGFP or with mock expression constructs. After 48 h of transfection, cell extracts were prepared and analyzed as described for panel E.

Polι. We therefore examined the expression of both variant Polι and Polη in the absence or presence of UV irradiation by Western blotting. As shown in Fig. 3A and B, exposure to UV did not restore the stability of variant Polι or increase Polη expression, indicating that the amount of variant Polι protein that exists in 129-derived fibroblasts is sufficient to cope with UV-induced DNA damage. Finally, similar sensitivities were observed in all genotypes when fibroblasts were exposed to hydrogen peroxide (H_2O_2), methyl methanesulfonate (MMS), and mitomycin C (MMC) (see Fig. S2C to E). Because MEFs tested for UV sensitivity have a different genetic background (mixed C57Bl/6x 129 backgrounds for gene-targeted strains compared to pure C57BL/6 and 129/Ola strains), we wanted to confirm that the UV sensitivity of *Polι*$^{-/-}$ fibroblasts resulted from the absence of Polι under isogenic conditions. To this end, we stably transfected immortalized *Polι*$^{-/-}$ fibroblasts with an expression vector encoding either a full-length wt protein or variant Polι protein. We selected two different clones giving positive results that expressed the exogenous protein at a level close to that of the endogenous protein (data not shown). We then assessed the sensitivity of these clones following exposure to UV radiation in the presence of caffeine. As shown in Fig. 4A, both wt Polι and variant Polι fully rescued the UV sensitivity of *Polι*$^{-/-}$ cells, with only small variations observed among the different clones. Furthermore, expression of a catalytically inactive form of Polι did not rescue the UV sensitivity of *Polι*$^{-/-}$ fibroblasts (Fig. 4B), indicating that the enzymatic activity of Polι, and not a scaffolding role for other TLS polymerases, is required to restore UV resistance. These results together support the hypothesis that the Polι variant corresponds to an active protein that is able to restore the ability of cells to tolerate UV-induced damage.

Variant Polι accumulates in nuclear replication foci after UV irradiation. Like Polη, Polι is reportedly associated with the replication machinery and accumulates as foci at replication forks

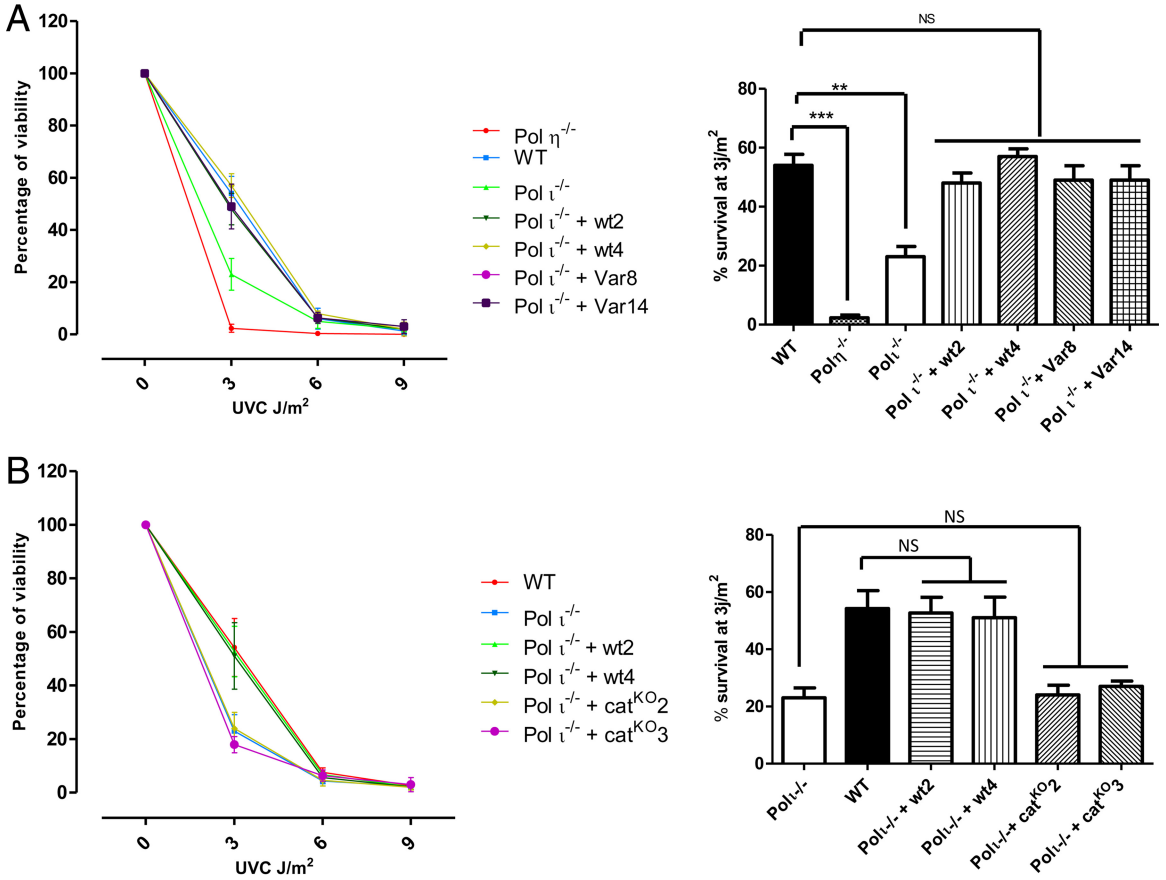

FIG 4 wt and variant Polι proteins, but not the catalytic mutant, complement the UV sensitivity of the Polι KO cell line. *Polι*$^{-/-}$ fibroblasts were stably transfected with wt Polι-eGFP, variant Polι-eGFP, or the Polι-eGFP D34A mutant. Two clones from each transfection with positive results were selected for this study. Cells were irradiated with different doses of UVC as indicated and grown for 72 h post-UV irradiation in medium supplemented with 1 mM caffeine. The surviving live-cell fraction was expressed as a percentage of the unirradiated cells (left panels). The right panels represent the fraction of live cells irradiated at 3 J/m^2 of UVC expressed as a percentage of total cells. Values are the means ± SD of the results of two independent experiments performed in triplicate (**, $P < 0.01$; ***, $P < 0.001$).

stalled by UV-induced DNA damage (20). To investigate the capacity of the eGFP-tagged Polι variant to localize in replication foci, we transiently transfected normal MRC5 fibroblasts with the corresponding expression vector. Thirty-six hours later, most soluble proteins were removed before fixation and immunostaining using an anti-PCNA antibody. We first verified that both wt and variant Polι-eGFP proteins were predominantly localized within the nucleus and appeared homogenously distributed in the absence of UV challenge (not shown), indicating that fusion with eGFP did not affect Polι localization within the cell. Six hours after application of 20 J/m^2 of UVC, both wt Polι and variant Polι formed detergent-resistant nuclear foci in most PCNA-positive cells (Fig. 3D). These data indicate that, similarly to wt Polι, the variant Polι isoform retained its capacity to localize and accumulate in nuclear foci after UVC irradiation.

Mouse strains derived from the 129 strain express an active Polι isoform. To assess whether the Polι variant retains the ability to incorporate deoxynucleoside triphosphates (dNTPs), we took advantage of the selective increase in Polι catalytic activity in the presence of manganese to address its polymerization activity using an in-gel activity assay (18). Starting with a protein mixture, this technique enables the enzymatic activity of a given protein to be assayed following SDS-PAGE in the presence of activated DNA. Crude extracts from mouse testes were either directly loaded into 10% polyacrylamide gels containing activated DNA (Fig. 3E) or subjected to immunoprecipitation using anti-Polι antibodies prior to loading (Fig. 3F). In-gel activity analysis was then conducted after protein renaturation. The resulting autoradiogram showed that no dNTP incorporation was observed for testis extracts of Polι$^{-/-}$ mice at the expected size of the enzyme, whereas activity was clearly detected in extracts from both wt (C57BL/6 and BALB/c) and variant Polι (129/Ola) mice. Similarly, both immunoprecipitated proteins maintained polymerase activity, although no activity was detected in the protein complex immunoprecipitated from *Polι*$^{-/-}$ mice (Fig. 3E and F). Finally, to unequivocally show that the observed activity was displayed by both isoforms of the enzyme, we transfected *Polι*$^{-/-}$ fibroblasts with empty vector or wt Polι-eGFP-expressing or variant Polι-eGFP-expressing plasmids prior to the in-gel activity analysis. Both expressed isoforms exhibited DNA polymerase activity (Fig. 3G). These findings clearly indicate that 129-derived mouse strains express a Polι enzyme lacking the exon 2-encoded domain and that this enzyme retains the ability to incorporate dNTPs in the presence of manganese.

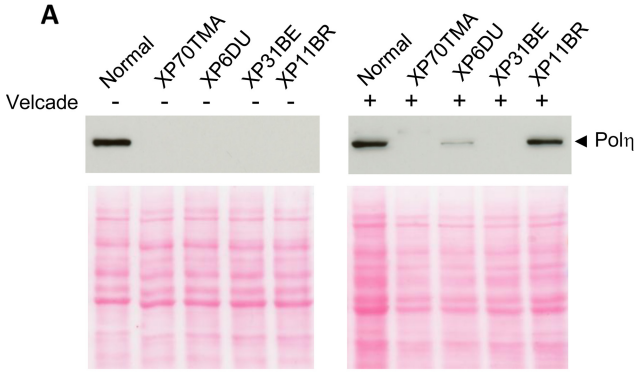

C

Cell strain	Genomic mutation (exon)	Amino-acid change	Cancer type
XP70TMA	c.454 C>T (4)	Gln152X	cutaneous squamous and basal cell carcinomas*
XP6DU	c. 224-226 del (3) c. G 207 (3)	- Leu75 fs69	high incidence of skin cancers**
XP31DU	c.764+1G>C (6)	Val221Profs	cutaneous squamous cell carcinomas, basal cell carcinomas and cutaneous melanomas *
XP11BR	c. 788 G>T (6)	Gly263Val	high incidence of skin cancers**

The DNA numbering system is based on the cDNA sequence of the *POLH* gene (MN_006502.2)
* from Corriell Institute for Medical Research database
** from Broughton et al. (2002)

FIG 5 Accumulation of mutant Polη protein upon the inhibition of the proteasome in transformed skin fibroblasts from XPV patients. Normal fibroblasts (from healthy donors) and XPV fibroblasts were grown in the presence or absence of Velcade. Following 3 h of treatment, whole-cell extracts were prepared, and the expression of Polη was estimated using Western blot analysis. Ponceau S Red staining served as a loading control. (B) Schematic representation of human Polη. PAD, polymerase-associated domain (little finger); UBZ, ubiquitin-binding zinc finger; NLS, nuclear localization signal; PIP, PCNA-interacting peptide box. The position of each mutation is indicated. (C) Description of the mutations found in the *POLH* gene of the XPV patients analyzed in this study and the associated cancer types. Broughton et al. (2002), reference 45.

Proteasomal degradation of functional Polη in XPV fibroblasts. DNA Polη is another member of the Y family of TLS DNA polymerases, and the major biological function of this protein is to enable accurate replication across UV irradiation-induced cyclobutane pyrimidine dimers. The absence of this protein causes XPV syndrome in humans. Recently, an analysis of a large cohort of XPV patients showed that, in most cases, the Polη protein was undetectable in patients' fibroblasts (21), even in the case of missense mutations. Therefore, we analyzed the expression of Polη in the presence of a proteasome inhibitor. Four cell lines were selected for this study: XP70TMA (with a homozygote nonsense mutation [Gln152X]), XP6DU (with a 1-amino-acid [aa] deletion in one allele [delLeu75] and a frameshift at K69 [Lys69fs] due to a deletion of a G at nucleotide 207 in the second allele), XP11BR (with a homozygous missense mutation [Gly263Val]), and XP31BE (with a homozygous change of G to C at an exon 6 splice donor site leading to total [104-bp] or partial [42-bp] deletion of exon 6 [Val221Profs]). In the absence of Velcade, Polη protein was undetectable in all four XPV cell lines (Fig. 5). In the presence of Velcade, however, a clear band corresponding to Polη was detected in the XP6DU and XP11BR cell lines and remained undetectable in XP70TMA and XP31BE, indicating that proteasomal degradation accounts for the low expression levels of *POLH* missense mutants.

We and others have previously shown that Polη is a mutagenic polymerase that is recruited during the Ig gene hypermutation process and that this polymerase is a major contributor to mutations at A/T base pairs (19, 22). Interestingly, Polκ acts as a replacement polymerase in the absence of Polη (23). The contribution of each enzyme is easily identified by its mutation signature: transversions for Polκ and transitions for Polη. However, Polκ acts only in the complete absence of Polη because mutating B cells with reduced Polη levels still harbor the typical transition mutation pattern of Polη (23). The Ig gene mutation patterns of memory B cells from XP11BR and XP31BE patients (as well as from XP7BR patients, whose genomic *POLH* mutations are identical to those of the XP6DU patients studied here) have been reported previously (24, 25). Very strikingly, for patients with both *POLH* missense mutations (XP11BR and XP6DU), the mutation profile revealed a clear *POLH* transition signature, albeit with a reduced A/T mutation frequency, demonstrating that the residual protein is catalytically active (see Fig. S4 in the supplemental material). These results further explain and document a disease case in

which the genetic mutation results in the destabilization of a functional protein that can be rescued *in vitro* by proteasome inhibition.

DISCUSSION

For more than a decade, 129-derived strains of mice have been described as being deficient in DNA polymerase iota (15) and have therefore frequently been used as a model to investigate the physiological function of this enzyme. However, on the basis of an analytical assay designed to detect the unique mutagenic profile of Polι, Gening and colleagues (16) showed that in 129/J strain mice, Polι activity was detectable in brain extracts but not in testis. In this report, we provide extensive evidence showing that 129-derived strains are indeed not completely deficient in Polι but rather express a variant of the Polι protein that retains catalytic activity in a wide variety of tissues. We first showed that these mouse strains express a major Polι mRNA species corresponding to a splicing variant lacking exon 2, which lacks 126 nucleotides but has an open reading frame. This splicing variant has been previously reported for 129/SvJ mice but has not been described as the most abundant Polι-encoding mRNA in this strain (10). Although the presence of a premature termination codon (PTC) is expected to lead to nonsense-mediated mRNA decay (NMD), a pathway that degrades mRNAs harboring PTCs, RNA analysis demonstrated that for mutated *Polι* RNA, the PTC mutation resulted in exon 2 skipping, a phenomenon corresponding to nonsense-associated altered splicing (26, 27). Exon skipping associated with PTCs is often explained by a structural effect on exon definition, by which the mutation alters the function of exonic splicing enhancers or silencers or of a *cis* determinant of exon identification (28, 29). Because the PTC is located early in the protein, this nonsense-associated altered splicing prevents the production of deleterious truncated proteins from PTC-harboring transcripts and provides the cell with an alternative isoform that can produce a functional protein.

Next, we showed that this exon 2-deficient mRNA is translated into a polypeptide, which was unambiguously identified using mass spectrometry, thus demonstrating that 129-derived mouse strains express a Polι variant protein that lacks the 42 amino acids encoded by exon 2. However, we observed that the variant protein was expressed at considerably lower steady-state levels in 129-derived mouse cells than in their wt counterparts. We established that this was due to the shorter half-life of the variant Polι resulting from its increased turnover. Finally, we showed that the Polι variant is directly ubiquitylated and that the variant can be stabilized in the presence of proteasome inhibitor, which indicates that the restricted accumulation of the Polι variant is due to proteasomal degradation.

With the aim of restoring the protein levels of the Polι variant *in vivo*, 129/Ola mice were treated with Velcade, which stably but reversibly inhibits the chymotryptic enzyme activity of the proteasome (Velcade has been approved for the treatment of multiple myeloma and mantle cell lymphoma). Treatment with Velcade results in a dramatic increase in variant Polι protein accumulation *in vivo*, a surprising observation that underscores the value of investigating the use of proteasome inhibitors to target diseases caused by the increased turnover of proteins with missense mutations.

Exon 2 skipping results in the deletion of a protein domain that has been described as indispensable for the activity of TLS polymerases because it is part of the conserved palm domain (3, 30). To assess whether the variant Polι is a functional TLS, we established a mouse strain in which the *Polι* gene was completely inactivated and compared the sensitivity of this strain to UVC-induced DNA damage with that of Polι-deficient fibroblasts from the 129 background. Interestingly, Polι-deficient cells showed a clear survival defect after UV irradiation, although this was less marked than that observed in Polη-deficient cells; in contrast, 129-derived fibroblasts behaved similarly to wt cells. Moreover, the transfection of variant Polι expression vectors fully rescued the UV sensitivity of Polι-deficient cells. We also showed that the variant Polι protein accumulates in repair/replication foci after UV irradiation, as reported for other TLS polymerases, and that the variant has clear Mn^{2+}-dependent deoxynucleotide polymerase activity, as demonstrated using in-gel polymerization assays. Moreover, using a cell-based assay, we showed that the expression of both wt and variant Polι proteins in *Polι*$^{-/-}$ fibroblasts was able to complement their UV tolerance defect, while the expression of full-length Polι with its catalytic site mutated could not correct their UV sensitivity. These data collectively document the involvement of Polι activity in the UV-generated DNA damage response and its cooperation with other TLS polymerases to maintain genome stability. The data also unambiguously demonstrate that 129-derived mouse cells are not Polι deficient and are thus an improper model for the study of cancer susceptibility linked to its absence.

Polη is another member of the Y polymerase family and is responsible for the error-free bypass of UV-induced cyclobutane pyrimidine dimers (31–34). Polη is also a major partner of the Ig gene hypermutation process and is responsible for mutations generated at A/T bases during the error-prone repair process taking place at the locus (13, 19, 35). Polη is the only TLS enzyme for which gene inactivation has been described in humans, a genetic deficiency that corresponds to the variant form of XPV (33, 36). In several cases of missense *POLH* mutations, an analysis of the patient's fibroblasts failed to detect protein expression and the mutated position did not have an obvious deleterious impact (21). By performing a protein analysis in the presence of proteasome inhibitor, we observed the accumulation of *POLH* missense mutants in XPV fibroblasts. Moreover, we previously discussed the observation that the pattern of Ig gene hypermutation in these XPV patients appears to conserve a clear Polη signature, which supports the notion that the residual protein, which is upregulated in activated B cells, retains catalytic activity (23). As observed for the variant Polι isoform, these *POLH* missense mutants fail to accumulate due to proteasomal degradation. The resulting XPV syndrome is thus caused by protein destabilization rather than functional inactivation.

In conclusion, the data collected in this study add to numerous reports of human diseases that are related to the ubiquitin-mediated turnover of misfolded proteins (37). Several genetic diseases corresponding to missense variants that are targeted by the ubiquitin-proteasome pathway, including cystic fibrosis, congenital erythropoietic porphyria, neurofibromatosis, Lynch syndrome, classic late-infantile neuronal ceroid lipofuscinosis, multiple endocrine neoplasia type 1, α-1 antitrypsin deficiency, and phenylketonuria, have been described previously (38–44). In several of the described cases, the destabilized mutant protein may nevertheless retain substantial functional properties. Thus, the development of tools that allow the specific targeting of proteasomal activity or of

the ubiquitin pathway to stabilize a protein variant might represent a promising approach for therapy.

ACKNOWLEDGMENTS

We thank the Gene Trap consortium for obtaining Polι-deficient ES cells and the SEAT (Villejuif) for the generation of Polι$^{-/-}$ mice. We also gratefully acknowledge Janssen-Cilag for providing us with Velcade. We acknowledge François Guillonneau, Plateau Protéome Université Paris Descartes, for his help with the MS/MS analysis.

This study was supported by the Fondation pour la Recherche Médicale and the Fondation Gustave Roussy. The Team "Développement du système immunitaire" is supported by the Ligue contre le Cancer (Equipe labelisée) and the Fondation Princesse Grace.

We declare that we have no conflicts of interest.

REFERENCES

1. **Ohmori H, Friedberg EC, Fuchs RP, Goodman MF, Hanaoka F, Hinkle D, Kunkel TA, Lawrence CW, Livneh Z, Nohmi T, Prakash L, Prakash S, Todo T, Walker GC, Wang Z, Woodgate R.** 2001. The Y-family of DNA polymerases. Mol Cell **8:**7–8. http://dx.doi.org/10.1016/S1097-2765(01)00278-7.
2. **Zhang Y, Yuan F, Wu X, Wang Z.** 2000. Preferential incorporation of G opposite template T by the low-fidelity human DNA polymerase iota. Mol Cell Biol **20:**7099–7108. http://dx.doi.org/10.1128/MCB.20.19.7099-7108.2000.
3. **Johnson RE, Washington MT, Haracska L, Prakash S, Prakash L.** 2000. Eukaryotic polymerases iota and zeta act sequentially to bypass DNA lesions. Nature **406:**1015–1019. http://dx.doi.org/10.1038/35023030.
4. **Tissier A, McDonald JP, Frank EG, Woodgate R.** 2000. poliota, a remarkably error-prone human DNA polymerase. Genes Dev **14:**1642–1650.
5. **Frank EG, Woodgate R.** 2007. Increased catalytic activity and altered fidelity of human DNA polymerase iota in the presence of manganese. J Biol Chem **282:**24689–24696. http://dx.doi.org/10.1074/jbc.M702159200.
6. **Choi J-H, Besaratinia A, Lee D-H, Lee C-S, Pfeifer GP.** 2006. The role of DNA polymerase iota in UV mutational spectra. Mutat Res **599:**58–65. http://dx.doi.org/10.1016/j.mrfmmm.2006.01.003.
7. **Dumstorf CA, Clark AB, Lin Q, Kissling GE, Yuan T, Kucherlapati R, McGregor WG, Kunkel TA.** 2006. Participation of mouse DNA polymerase iota in strand-biased mutagenic bypass of UV photoproducts and suppression of skin cancer. Proc Natl Acad Sci U S A **103:**18083–18088. http://dx.doi.org/10.1073/pnas.0605247103.
8. **Yang J, Chen Z, Liu Y, Hickey RJ, Malkas LH.** 2004. Altered DNA polymerase iota expression in breast cancer cells leads to a reduction in DNA replication fidelity and a higher rate of mutagenesis. Cancer Res **64:**5597–5607. http://dx.doi.org/10.1158/0008-5472.CAN-04-0603.
9. **Lee G-H, Nishimori H, Sasaki Y, Matsushita H, Kitagawa T, Tokino T.** 2003. Analysis of lung tumorigenesis in chimeric mice indicates the Pulmonary adenoma resistance 2 (Par2) locus to operate in the tumor-initiation stage in a cell-autonomous manner: detection of polymorphisms in the Poli gene as a candidate for Par2. Oncogene **22:**2374–2382. http://dx.doi.org/10.1038/sj.onc.1206387.
10. **Wang M, Devereux TR, Vikis HG, McCulloch SD, Holliday W, Anna C, Wang Y, Bebenek K, Kunkel TA, Guan K, You M.** 2004. Pol iota is a candidate for the mouse pulmonary adenoma resistance 2 locus, a major modifier of chemically induced lung neoplasia. Cancer Res **64:**1924–1931. http://dx.doi.org/10.1158/0008-5472.CAN-03-3080.
11. **Lee G-H, Matsushita H.** 2005. Genetic linkage between Pol iota deficiency and increased susceptibility to lung tumors in mice. Cancer Sci **96:**256–259. http://dx.doi.org/10.1111/j.1349-7006.2005.00042.x.
12. **Gueranger Q, Stary A, Aoufouchi S, Faili A, Sarasin A, Reynaud CA, Weill JC.** 2008. Role of DNA polymerases eta, iota and zeta in UV resistance and UV-induced mutagenesis in a human cell line. DNA Repair (Amst) **7:**1551–1562. http://dx.doi.org/10.1016/j.dnarep.2008.05.012.
13. **Wang Y, Woodgate R, McManus TP, Mead S, McCormick JJ, Maher VM.** 2007. Evidence that in xeroderma pigmentosum variant cells, which lack DNA polymerase eta, DNA polymerase iota causes the very high frequency and unique spectrum of UV-induced mutations. Cancer Res **67:**3018–3026. http://dx.doi.org/10.1158/0008-5472.CAN-06-3073.
14. **Ohkumo T, Kondo Y, Yokoi M, Tsukamoto T, Yamada A, Sugimoto T, Kanao R, Higashi Y, Kondoh H, Tatematsu M, Masutani C, Hanaoka F.** 2006. UV-B radiation induces epithelial tumors in mice lacking DNA polymerase eta and mesenchymal tumors in mice deficient for DNA polymerase iota. Mol Cell Biol **26:**7696–7706. http://dx.doi.org/10.1128/MCB.01076-06.
15. **McDonald JP, Frank EG, Plosky BS, Rogozin IB, Masutani C, Hanaoka F, Woodgate R, Gearhart PJ.** 2003. 129-derived strains of mice are deficient in DNA polymerase iota and have normal immunoglobulin hypermutation. J Exp Med **198:**635–643. http://dx.doi.org/10.1084/jem.20030767.
16. **Gening LV, Makarova AV, Malashenko AM, Tarantul VZ.** 2006. A false note of DNA polymerase iota in the choir of genome caretakers in mammals. Biochemistry (Mosc) **71:**155–159. http://dx.doi.org/10.1134/S0006297906020064.
17. **Newcomb EW, Diamond LE, Sloan SR, Corominas M, Guerrerro I, Pellicer A.** 1989. Radiation and chemical activation of ras oncogenes in different mouse strains. Environ Health Perspect **81:**33–37. http://dx.doi.org/10.1289/ehp.898133.
18. **Karawya E, Swack J, Albert W, Fedorko J, Minna JD, Wilson SH.** 1984. Identification of a higher molecular weight DNA polymerase alpha catalytic polypeptide in monkey cells by monoclonal antibody. Proc Natl Acad Sci U S A **81:**7777–7781. http://dx.doi.org/10.1073/pnas.81.24.7777.
19. **Delbos F, De Smet A, Faili A, Aoufouchi S, Weill J-C, Reynaud C-A.** 2005. Contribution of DNA polymerase eta to immunoglobulin gene hypermutation in the mouse. J Exp Med. **201:**1191–1196. http://dx.doi.org/10.1084/jem.20050292.
20. **Kannouche P, Fernández de Henestrosa AR, Coull B, Vidal AE, Gray C, Zicha D, Woodgate R, Lehmann AR.** 2003. Localization of DNA polymerases eta and iota to the replication machinery is tightly co-ordinated in human cells. EMBO J **22:**1223–1233. http://dx.doi.org/10.1093/emboj/7595006.
21. **Inui H, Oh KS, Nadem C, Ueda T, Khan SG, Metin A, Gozukara E, Emmert S, Slor H, Busch DB, Baker CC, DiGiovanna JJ, Tamura D, Seitz CS, Gratchev A, Wu WH, Chung KY, Chung HJ, Azizi E, Woodgate R, Schneider TD, Kraemer KH.** 2008. Xeroderma pigmentosum-variant patients from America, Europe, and Asia. J Investig Dermatol **128:**2055–2068. http://dx.doi.org/10.1038/jid.2008.48.
22. **Martomo SA, Yang WW, Wersto RP, Ohkumo T, Kondo Y, Yokoi M, Masutani C, Hanaoka F, Gearhart PJ.** 2005. Different mutation signatures in DNA polymerase eta- and MSH6-deficient mice suggest separate roles in antibody diversification. Proc Natl Acad Sci U S A **102:**8656–8661. http://dx.doi.org/10.1073/pnas.0501852102.
23. **Faili A, Stary A, Delbos F, Weller S, Aoufouchi S, Sarasin A, Weill JC, Reynaud CA.** 2009. A backup role of DNA polymerase kappa in Ig gene hypermutation only takes place in the complete absence of DNA polymerase eta. J Immunol **182:**6353–6359. http://dx.doi.org/10.4049/jimmunol.0900177.
24. **Zeng X, Winter DB, Kasmer C, Kraemer KH, Lehmann AR, Gearhart PJ.** 2001. DNA polymerase eta is an A-T mutator in somatic hypermutation of immunoglobulin variable genes. Nat Immunol **2:**537–541. http://dx.doi.org/10.1038/88740.
25. **Mayorov VI, Rogozin IB, Adkison LR, Gearhart PJ.** 2005. DNA polymerase eta contributes to strand bias of mutations of A versus T in immunoglobulin genes. J Immunol **174:**7781–7786. http://dx.doi.org/10.4049/jimmunol.174.12.7781.
26. **Valentine CR.** 1998. The association of nonsense codons with exon skipping. Mutat Res **411:**87–117. http://dx.doi.org/10.1016/S1383-5742(98)00010-6.
27. **Maquat LE.** 2002. NASty effects on fibrillin pre-mRNA splicing: another case of ESE does it, but proposals for translation-dependent splice site choice live on. Genes Dev **16:**1743–1753. http://dx.doi.org/10.1101/gad.1014502.
28. **Zhang XH-F, Kangsamaksin T, Chao MSP, Banerjee JK, Chasin LA.** 2005. Exon inclusion is dependent on predictable exonic splicing enhancers. Mol Cell Biol **25:**7323–7332. http://dx.doi.org/10.1128/MCB.25.16.7323-7332.2005.
29. **Liu HX, Cartegni L, Zhang MQ, Krainer AR.** 2001. A mechanism for exon skipping caused by nonsense or missense mutations in BRCA1 and other genes. Nat Genet **27:**55–58. http://dx.doi.org/10.1038/83762.
30. **Nair DT, Johnson RE, Prakash S, Prakash L, Aggarwal A. K.** 2004. Replication by human DNA polymerase-iota occurs by Hoogsteen base-pairing. Nature **430:**377–380. http://dx.doi.org/10.1038/nature02692.
31. **Johnson RE, Prakash S, Prakash L.** 1999. Efficient bypass of a thymine-

thymine dimer by yeast DNA polymerase, Poleta. Science **283:**1001–1004. http://dx.doi.org/10.1126/science.283.5404.1001.
32. **Washington MT, Johnson RE, Prakash S, Prakash L.** 1999. Fidelity and processivity of Saccharomyces cerevisiae DNA polymerase eta. J Biol Chem **274:**36835–36838. http://dx.doi.org/10.1074/jbc.274.52.36835.
33. **Masutani C, Kusumoto R, Yamada A, Dohmae N, Yokoi M, Yuasa M, Araki M, Iwai S, Takio K, Hanaoka F.** 1999. The XPV (xeroderma pigmentosum variant) gene encodes human DNA polymerase eta. Nature **399:**700–704. http://dx.doi.org/10.1038/21447.
34. **McCulloch SD, Kokoska RJ, Masutani C, Iwai S, Hanaoka F, Kunkel TA.** 2004. Preferential cis-syn thymine dimer bypass by DNA polymerase eta occurs with biased fidelity. Nature **428:**97–100. http://dx.doi.org/10.1038/nature02352.
35. **Delbos F, Aoufouchi S, Faili A, Weill J-C, Reynaud C-A.** 2007. DNA polymerase eta is the sole contributor of A/T modifications during immunoglobulin gene hypermutation in the mouse. J Exp Med **204:**17–23. http://dx.doi.org/10.1084/jem.20062131.
36. **Johnson RE, Kondratick CM, Prakash S, Prakash L.** 1999. hRAD30 mutations in the variant form of xeroderma pigmentosum. Science **285:**263–265. http://dx.doi.org/10.1126/science.285.5425.263.
37. **Winklhofer KF, Tatzelt J, Haass C.** 2008. The two faces of protein misfolding: gain- and loss-of-function in neurodegenerative diseases. EMBO J **27:**336–349. http://dx.doi.org/10.1038/sj.emboj.7601930.
38. **Blouin J-M, Duchartre Y, Costet P, Lalanne M, Ged C, Lain A, Millet O, de Verneuil H, Richard E.** 2013. Therapeutic potential of proteasome inhibitors in congenital erythropoietic porphyria. Proc Natl Acad Sci U S A **110:**18238–18243. http://dx.doi.org/10.1073/pnas.1314177110.
39. **Gautreau A.** 2002. Mutant products of the NF2 tumor suppressor gene are degraded by the ubiquitin-proteasome pathway. J Biol Chem **277:**31279–31282. http://dx.doi.org/10.1074/jbc.C200125200.
40. **Arlow T, Scott K, Wagenseller A, Gammie A.** 2013. Proteasome inhibition rescues clinically significant unstable variants of the mismatch repair protein Msh2. Proc Natl Acad Sci **110:**246–251.
41. **Walus M, Kida E, Golabek AA.** 2010. Functional consequences and rescue potential of pathogenic missense mutations in tripeptidyl peptidase I. Hum Mutat **31:**710–721. http://dx.doi.org/10.1002/humu.21251.
42. **Yaguchi H, Ohkura N, Takahashi M, Nagamura Y, Kitabayashi I, Tsukada T.** 2004. Menin missense mutants associated with multiple endocrine neoplasia type 1 are rapidly degraded via the ubiquitin-proteasome pathway. Mol Cell Biol **24:**6569–6580. http://dx.doi.org/10.1128/MCB.24.15.6569-6580.2004.
43. **Kroeger H, Miranda E, MacLeod I, Pérez J, Crowther DC, Marciniak SJ, Lomas DA.** 2009. Endoplasmic reticulum-associated degradation (ERAD) and autophagy cooperate to degrade polymerogenic mutant serpins. J Biol Chem **284:**22793–22802. http://dx.doi.org/10.1074/jbc.M109.027102.
44. **Shi Z, Sellers J, Moult J.** 2012. Protein stability and in vivo concentration of missense mutations in phenylalanine hydroxylase. Proteins **80:**61–70. http://dx.doi.org/10.1002/prot.23159.
45. **Broughton BC, Cordonnier A, Kleijer WJ, Jaspers NG, Fawcett H, Raams A, Garritsen VH, Stary A, Avril MF, Boudsocq F, Masutani C, Hanaoka F, Fuchs RP, Sarasin A, Lehmann AR.** 2002. Molecular analysis of mutations in DNA polymerase eta in xeroderma pigmentosum-variant patients. Proc Natl Acad Sci U S A **99:**815–820. http://dx.doi.org/10.1073/pnas.022473899.